

Effective Dielectric Constants of Photonic Crystal of Aligned Anisotropic Cylinders: Application to the Optical Response of Periodic Array of Carbon Nanotubes

E. Reyes¹, A.A. Krokhin², and J. Roberts²

¹*Instituto de Física, Universidad Autónoma de Puebla,*

Apartado Postal J-48, Puebla, 72570 Mexico and

²*Department of Physics, University of North Texas,*

P.O. Box 311427, Denton, TX 76203

(Dated: July 27, 2021)

We calculate the static dielectric tensor of a periodic system of aligned anisotropic dielectric cylinders. Exact analytical formulas for the effective dielectric constants for the E - and H - eigenmodes are obtained for arbitrary 2D Bravais lattice and arbitrary cross-section of anisotropic cylinders. It is shown that depending on the symmetry of the unit cell photonic crystal of anisotropic cylinders behaves in the low-frequency limit like uniaxial or biaxial natural crystal. The developed theory of homogenization of anisotropic cylinders is applied for calculations of the dielectric properties of photonic crystals of carbon nanotubes.

PACS numbers:

42.70.Qs, 41.20.Jb, 42.25.Lc

I. INTRODUCTION

Periodic dielectric structures - photonic crystals (PC) - have found many useful technological applications.¹ Progress in the development of optical devices that operate using the principles of the control of light as proposed by Yablonovich² gave rise to theoretical studies of the general properties of the spectra of PC's.³ In particular, the region of low frequencies, where the ideas and methods of the theory of homogenization⁴ are applicable, has attracted a significant amount of attention in the last decade. In the low-frequency limit the light wave in a non-absorbable periodic medium has linear dispersion, $\omega \propto k$. This allows the

replacement a real inhomogeneous medium by an effective homogeneous one with dielectric permittivity

$$\epsilon_{eff}(\hat{\mathbf{k}}) = \lim_{k \rightarrow 0} \left(\frac{ck}{\omega} \right)^2. \quad (1)$$

In the general case, this effective parameter depends on the direction of propagation $\hat{\mathbf{k}} = \mathbf{k}/k$ and has tensor structure. The latter property is emphasized for 2D PC's, which are anisotropic uniaxial or biaxial crystals, depending on the symmetry of the unit cell.⁵ Unlike this, 3D PC's may be isotropic.⁶

Optical anisotropy of the PC's studied in Refs. [5,6,7] is determined by the geometry of the unit cell only. The constituents themselves are considered to be isotropic dielectrics. This is not the case, for example, for a structure of aligned carbon nanotubes arranged periodically in the plane perpendicular to the tubes. Here anisotropy manifests itself at the "microscopic" level, since the nanotubes ("atoms" of the PC) possess a natural anisotropy. This anisotropy originates from the layered structure of the crystal of graphite, which has different dielectric constants along the c -axis and in the perpendicular plane. The static values of these dielectric constants are $\epsilon_{\parallel} = 1.8225$ and $\epsilon_{\perp} = 5.226$.¹⁵ The elongated topology and the natural anisotropy of graphite cause PC's of carbon nanotubes to exhibit large optical anisotropy.⁸ Three-dimensional PC's with anisotropic dielectric spheres have been studied in Refs.[9]. It was shown, that, depending on the symmetry of the unit cell, the anisotropy of the spheres may be favorable for either broadening or narrowing the band gaps.

High anisotropy of 2D photonic crystals may find interesting applications in nanophotonics as it was recently proposed by Artigas and Torner.¹⁰ Namely, the surface of an anisotropic 2D photonic crystal supports propagation of a surface wave predicted by Dyakonov.¹¹ The surface mode does not radiate and is localized close to the surface due to the interference between the ordinary and extraordinary waves. In natural crystals, it can be hardly observed because of the low anisotropy. Since it is a surface wave with very low energy losses, the Dyakonov wave may replace surface plasmons in the near-field optics and integrated photonic circuits.

An effective medium theory for the PC of anisotropic carbon nanotubes was proposed in Ref. [12]. This theory is based on the Maxwell-Garnet approximation.¹³ and it leads to a simple analytical formula for the effective dielectric constant. The formula is valid at low

filling fractions. Since the Maxwell-Garnett approximation does not discriminate between periodic and non-periodic arrangements of the nanotubes, the in-plane anisotropy of the effective dielectric constant is lost. In other words, ε_{eff} in Eq. (1) is independent on $\hat{\mathbf{k}}$, i.e., the Maxwell-Garnett approximation always leads to an effective medium which is equivalent to a uniaxial crystal. The PC considered in Ref. [12] has a square unit cell that gives rise to in-plane isotropy of the effective dielectric tensor.

In this paper we extend the results of the theory of homogenization⁵ to the case of anisotropic dielectric cylinders. Exact analytical formulas are obtained for the principal effective dielectric constants of a 2D PC with an arbitrary cross-sectional form of anisotropic cylinders, arbitrary Bravais lattice, and filling fraction. We compare our results with the results obtained for the PC of carbon nanotubes in the modified Maxwell-Garnett approximation.¹² This comparison shows that the Maxwell-Garnett approximation gives correct results for a dilute system with filling fraction less than 5%. However, at higher filling fractions the Maxwell-Garnett approximation overestimates the values for the effective dielectric constant. For a close-packed structure the error is about 10%. We also consider a PC with a rectangular unit cell and calculate two different in-plane dielectric constants. In this case the corresponding effective medium is a biaxial crystal. It was argued that for the H -polarized mode the effective dielectric constant for hollow and solid cylinders are practically indistinguishable.¹² Using our approach, we study the effect of the internal cavity on the effective dielectric constant and show explicitly how the effective dielectric constant decreases with the internal radius.

II. THE FOURIER EXPANSION METHOD IN THE LONG-WAVELENGTH LIMIT

We consider a 2D periodic structure of dielectric cylinders with their axes parallel to z and whose cross section can have an arbitrary shape. The cylinders are imbedded in a dielectric matrix. A 2D PC supports propagation of two uncoupled modes with either E -polarization (where the vector \mathbf{E} is parallel to the cylinders), or H -polarization (in this case the vector \mathbf{H} is parallel to the cylinders). The background material is an isotropic dielectric with permittivity ε_b and the cylinders are rolled up from an anisotropic dielectric sheet characterized by a tensor $\hat{\varepsilon}^{(a)}$. For carbon nanotubes, this tensor has two different

eigenvalues, and in cylindrical coordinates is represented by a diagonal matrix with elements $\varepsilon_{\theta\theta}^{(a)} = \varepsilon_{zz}^{(a)} = \varepsilon_{\perp}$ and $\varepsilon_{rr}^{(a)} = \varepsilon_{\parallel}$. As a whole, the periodic inhomogeneous dielectric medium is characterized by the coordinate-dependent dielectric tensor,

$$\hat{\varepsilon}(\mathbf{r}) = \begin{pmatrix} \varepsilon_{xx}(\mathbf{r}) & \varepsilon_{xy}(\mathbf{r}) & 0 \\ \varepsilon_{yx}(\mathbf{r}) & \varepsilon_{yy}(\mathbf{r}) & 0 \\ 0 & 0 & \varepsilon_{zz}(\mathbf{r}) \end{pmatrix}. \quad (2)$$

Inside the cylinders this tensor coincides with $\hat{\varepsilon}^{(a)}$ and outside the cylinders it reduces to a scalar, $\varepsilon_b \delta_{ik}$.

The wave equations for the E - and H -polarized modes with frequency ω have the following form:

$$\nabla^2 E = \frac{\omega^2}{c^2} \varepsilon_{zz}(\mathbf{r}) E, \quad (3)$$

$$\frac{\partial}{\partial x_i} \left(a_{ji} \frac{\partial H}{\partial x_j} \right) + \frac{\omega^2}{c^2} H = 0, \quad x_i, x_j = x, y. \quad (4)$$

Here $E = E(x, y)$ and $H = H(x, y)$ are the amplitudes of the E and H monochromatic eigenmodes, respectively, and a_{ij} is a 2×2 Hermitian matrix with determinant 1:

$$a_{ij}(\mathbf{r}) = \frac{1}{\varepsilon_{xx}(\mathbf{r})\varepsilon_{yy}(\mathbf{r}) - \varepsilon_{xy}(\mathbf{r})\varepsilon_{yx}(\mathbf{r})} \begin{pmatrix} \varepsilon_{xx}(\mathbf{r}) & \varepsilon_{xy}(\mathbf{r}) \\ \varepsilon_{yx}(\mathbf{r}) & \varepsilon_{yy}(\mathbf{r}) \end{pmatrix}. \quad (5)$$

The determinant in the right-hand side can be written as a product of two eigenvalues. Within the graphite wall of the cylinders this product is $\varepsilon_{\parallel}\varepsilon_{\perp}$. Outside the wall it is either $(\varepsilon^{(b)})^2$ (for \mathbf{r} being outside the cylinders) or 1 for the interior region of the cylinder, which is free from the dielectric material.

Eq.(3) depends only on the zz component of the dielectric tensor, i.e., it is insensitive to the in-plane anisotropy. Therefore the effective dielectric constant in the long-wavelength limit is the same as for the parallel arrangement of isotropic cylinders (not necessarily periodic). It is given by a simple formula

$$\varepsilon_{eff}^{(E)} = \bar{\varepsilon}_{zz}, \quad (6)$$

where

$$\bar{\varepsilon}_{zz} = \frac{1}{A_c} \int_{A_c} \varepsilon_{zz}(\mathbf{r}) d\mathbf{r}, \quad (7)$$

is the average over the area A_c of the unit cell zz component of the tensor (2). For a binary composite $\varepsilon_{eff}^{(E)} = \bar{\varepsilon}_{zz} = f\varepsilon_{\perp} + (1-f)\varepsilon_b$, where f is the filling fraction of the component a .

To obtain the long-wavelength limit for Eq. (4) we apply the method of plane waves.⁵ Using the Bloch theorem and the periodicity of the function $a_{ij}(\mathbf{r})$, we get the Fourier expansions,

$$H(\mathbf{r}) = \exp(i\mathbf{k} \cdot \mathbf{r}) \sum_{\mathbf{G}} h_{\mathbf{k}}(\mathbf{G}) \exp(i\mathbf{G} \cdot \mathbf{r}), \quad (8)$$

$$a_{ij}(\mathbf{r}) = \sum_{\mathbf{G}} a_{ij}(\mathbf{G}) \exp(i\mathbf{G} \cdot \mathbf{r}), \quad (9)$$

where the Fourier coefficients $a_{ij}(\mathbf{G})$ are given by

$$\begin{aligned} a_{ij}(\mathbf{G}) &= \frac{1}{A_c} \int_{A_c} a_{ij}(\mathbf{r}) \exp(-i\mathbf{G} \cdot \mathbf{r}) d\mathbf{r} \\ &= \frac{1}{\varepsilon_{\parallel} \varepsilon_{\perp} A_c} \int_a \varepsilon_{ij}^{(a)}(\mathbf{r}) \exp(-i\mathbf{G} \cdot \mathbf{r}) d\mathbf{r} + \frac{\delta_{ij}}{A_c} \left[\frac{1}{\varepsilon_b^2} \int_b \exp(-i\mathbf{G} \cdot \mathbf{r}) d\mathbf{r} + \int_c \exp(-i\mathbf{G} \cdot \mathbf{r}) d\mathbf{r} \right]. \end{aligned} \quad (10)$$

Here \mathbf{G} gives the reciprocal-lattice vectors. Indices a , b , and c at the integrals label the domains of integration – within the graphite walls, within the dielectric matrix, and within the interior of the hollow cylinders respectively. Substituting Eqs. (8) and (9) into Eq. (4) we get a generalized eigenvalue problem in \mathbf{G} -space,

$$\sum_{\mathbf{G}'} a_{ij}(\mathbf{G} - \mathbf{G}') (\mathbf{k} + \mathbf{G})_i (\mathbf{k} + \mathbf{G}')_j h_{\mathbf{k}}(\mathbf{G}') = (\omega^2/c^2) h_{\mathbf{k}}(\mathbf{G}), \quad i, j = x, y. \quad (11)$$

Eq. (11) is an infinite set of homogeneous linear equations for the eigenfunctions $h_{\mathbf{k}}(\mathbf{G})$. The dispersion relation $\omega = \omega_n(\mathbf{k})$ ($n = 1, 2, \dots$) is obtained from the condition that this set has non-trivial solutions.

The periodic medium behaves as a homogeneous one if the Bloch wave (8) approaches a plane wave. This occurs if the Fourier coefficients with $\mathbf{G} \neq 0$ in (8) vanish in the long-wavelength limit. To obtain the behavior of $h_{\mathbf{k}}(\mathbf{G})$ we substitute $\mathbf{G} = 0$ in both sides of Eq. (11), divide the both sides by $h_{\mathbf{k}}(\mathbf{G} = 0)$ and take the limit as $k \rightarrow 0$

$$1 = \frac{1}{\omega^2/c^2 - \bar{a}_{ij} k_i k_j} \sum_{\mathbf{G}' \neq 0} a_{ij}(-\mathbf{G}') k_i G'_j h_{\mathbf{k}}^*(\mathbf{G}'). \quad (12)$$

Here $\bar{a}_{ij} \equiv a_{ij}(\mathbf{G} = 0)$ is the bulk average of the matrix (5) and $h_{\mathbf{k}}^*(\mathbf{G}) = h_{\mathbf{k}}(\mathbf{G})/h_{\mathbf{k}}(\mathbf{G} = 0)$ is the normalized Fourier coefficient. In the long-wavelength limit the coefficients of $h_{\mathbf{k}}^*(\mathbf{G}')$ in the right-hand side are inversely proportional to k . In order to make the sum finite, the amplitudes of non-zero harmonics, $h_{\mathbf{k}}^*(\mathbf{G}')$ must approach zero linearly with k . Thus, in the long-wavelength limit the Bloch wave (8) can be written as a linear expansion over powers of k :

$$H(\mathbf{r}) = \exp(i\mathbf{k} \cdot \mathbf{r}) \left[h_0 + \sum_{\mathbf{G} \neq 0} h_{\mathbf{k}}^*(\mathbf{G}) \exp(i\mathbf{G} \cdot \mathbf{r}) \right]. \quad (13)$$

Since the sum over \mathbf{G} vanishes linearly with k , Eq. (13) shows that the medium becomes homogeneous, i.e. the solution of the wave equation (4) approaches a plane wave with an amplitude $h_0 = h_{\mathbf{k}}(\mathbf{G} = 0)$ when $k \rightarrow 0$.

Now, to calculate the effective dielectric constant (1), we develop a theory of perturbation with respect to a small parameter ka (a is the lattice period). In Eq. (11) we keep the linear terms and obtain the following relation,

$$a_{ij}(\mathbf{G})G_i k_j + \sum_{\mathbf{G}' \neq \mathbf{0}} a_{ij}(\mathbf{G} - \mathbf{G}')G_i G'_j h_{\mathbf{k}}^*(\mathbf{G}') = 0. \quad (14)$$

The quadratic approximation is given by Eq. (12), which gives another linear relation between the eigenvectors $h_{\mathbf{k}}^*(\mathbf{G})$. Note that this relation is obtained from the eigenvalue problem Eq. (11) for $\mathbf{G} = 0$ and the linear approximation Eq. (14) is obtained for $\mathbf{G} \neq 0$. The linear relations, Eqs. (12) and (14), are the homogenized equations for the Fourier components of the magnetic field. These equations are consistent, if the corresponding determinant vanishes:

$$\det_{\mathbf{G}, \mathbf{G}' \neq \mathbf{0}} \left[\Lambda a_{ij}(\mathbf{G} - \mathbf{G}')G_i G'_j - a_{ij}(\mathbf{G})a_{mn}(-\mathbf{G}')G_i n_j n_m G'_n \right] = 0. \quad (15)$$

Here $\mathbf{n} = \mathbf{k}/k$ is the unit vector in the direction of propagation and $\Lambda = (\bar{a}_{ij}n_i n_j - \varepsilon_{eff}^{-1})$. Since Eqs. (12) and (14) are homogenous with respect to k , the dispersion equation (15) depends only on the inverse effective dielectric constant, $(\omega/c k)^2$. This fact is a manifestation of a general property: At low frequencies an electromagnetic wave has a linear dispersion in a periodic dielectric medium.

Although Eq. (15) is an infinite-order polynomial equation in Λ , it turns out that it has only a *unique* nonzero solution. The fact that the second term in the determinant Eq. (15) is a product of two factors, one of which depends only on \mathbf{G} and the other only on \mathbf{G}' , plays a crucial role. Omitting the mathematical details, which can be found in Ref. [5], we obtain the final answer for the inverse effective dielectric constant obtained from Eq. (15) as:

$$\frac{1}{\varepsilon_{eff}^{(H)}(\hat{\mathbf{n}})} = \bar{a}_{ij}n_i n_j - \sum_{\mathbf{G}, \mathbf{G}' \neq \mathbf{0}} a_{ij}(\mathbf{G})a_{mn}(-\mathbf{G}')n_j G_i n_m G'_n [a_{kl}(\mathbf{G} - \mathbf{G}')G_k G'_l]^{-1}. \quad (16)$$

Here $[\dots]^{-1}$ implies the inverse matrix in \mathbf{G} -space. Eq. (16) is valid for an arbitrary form of the unit cell, geometry of the cylindrical inclusions, material composition of the photonic crystal, and the direction of propagation in the plane of periodicity. In the case when $a_{ij}(\mathbf{G}) = \eta(\mathbf{G})\delta_{ij}$ Eq. (16) is reduced to the formula obtained for isotropic cylinders.⁵

III. INDEX ELLIPSOID

As any natural crystal, artificial PC in the long-wavelength limit can be characterized by an index ellipsoid.¹⁴ Taking into account Eq. (6) the equation for this ellipsoid can be written as follows:

$$\frac{x_0^2}{\varepsilon_1} + \frac{y_0^2}{\varepsilon_2} + \frac{z_0^2}{\bar{\varepsilon}_{zz}} = 1. \quad (17)$$

Here x_0, y_0, z_0 are three mutually orthogonal directions along which the vectors of the electric field, \mathbf{E} , and of the displacement, \mathbf{D} , are parallel to each other. For the E -mode we have $\mathbf{E} \parallel \mathbf{D} \parallel \hat{\mathbf{z}}$, i.e. the z_0 direction coincides with z -axis. In the $x - y$ plane the cross section of the index ellipsoid is given by Eq. (16), which can be rewritten in the canonical form as

$$\frac{1}{\varepsilon_{eff}^{(H)}(\varphi)} = (\bar{a}_{xx} - A_{xx}) \cos^2 \varphi + (\bar{a}_{yy} - A_{yy}) \sin^2 \varphi + (\bar{a}_{xy} - A_{xy}) \sin 2\varphi. \quad (18)$$

Here

$$A_{ij} = \sum_{\mathbf{G}, \mathbf{G}' \neq 0} a_{ik}(\mathbf{G}) a_{jl}(-\mathbf{G}') G_k G_l' [a_{mn}(\mathbf{G}' - \mathbf{G}) G_m G_n']^{-1}, \quad i, j, k, l, m, n = x, y. \quad (19)$$

Eq. (18) describes a rotated ellipse in the polar coordinates (ρ, φ) . The radius $\rho(\varphi) = \sqrt{\varepsilon_{eff}^{(H)}(\varphi)}$ gives the index of refraction of H -mode and the angle φ is related to the direction of propagation, $\hat{\mathbf{n}} = (\cos \varphi, \sin \varphi)$. The directions x_0 and y_0 coincide with the semi-axes of the ellipse given by Eq. (18) and the in-plane indices of refraction $\sqrt{\bar{\varepsilon}_1}, \sqrt{\bar{\varepsilon}_2}$ are given by the lengths of the semi-axes. The angle of rotation of the axes of the ellipse Eq. (18) with respect to the arbitrary axes x, y , is given by the relation

$$\tan(2\theta) = \frac{2A_{xy}}{A_{yy} - A_{xx}}. \quad (20)$$

If the unit cell possesses a third- or higher-order rotational axis z , then the tensor A_{ij} is reduced to a scalar, $A_{ij} = A\delta_{ij}$, and the ellipse given by Eq. (18) is reduced to a circle. In this case the PC in the long-wavelength limit behaves like a uniaxial crystal; otherwise, it is biaxial.

IV. UNIAXIAL AND BIAxIAL PC'S OF SOLID GRAPHITE CYLINDERS

In this section, we study 2D PC of solid carbon cylinders arranged in square and rectangular lattices. In Cartesian coordinates the dielectric function of a carbon cylinder is given

by the tensor¹²

$$\hat{\varepsilon}^{(a)}(\mathbf{r}) = \begin{pmatrix} \frac{x^2}{r^2}\varepsilon_{\parallel} + \frac{y^2}{r^2}\varepsilon_{\perp} & \frac{xy}{r^2}(\varepsilon_{\parallel} - \varepsilon_{\perp}) & 0 \\ \frac{xy}{r^2}(\varepsilon_{\parallel} - \varepsilon_{\perp}) & \frac{y^2}{r^2}\varepsilon_{\parallel} + \frac{x^2}{r^2}\varepsilon_{\perp} & 0 \\ 0 & 0 & \varepsilon_{\perp} \end{pmatrix}. \quad (21)$$

In numerical calculations we use Eq. (18) and (19). For rectangular and square lattices with circular cylinders the semi-axes of the index ellipsoid are directed along the basic lattice vectors. Because of the high symmetry of the unit cell, the off-diagonal elements of the tensor $a_{ik}(\mathbf{G})$ vanish. The diagonal elements for hollow cylinders with outer and inner radii R and γR , respectively, ($0 \leq \gamma \leq 1$) have the following form:

$$a_{xx}(\mathbf{G}) = \begin{cases} \frac{\pi R^2}{A_c} \left[\frac{1}{2} (\varepsilon_{\parallel}^{-1} + \varepsilon_{\perp}^{-1}) (1 - \gamma^2) \right] + \varepsilon_b^{-1} (1 - \frac{\pi R^2}{A_c} (1 - \gamma^2)), & \mathbf{G} = 0, \\ \frac{2\pi}{A_c G^2} \left\{ GR (\varepsilon_{\perp}^{-1} - \varepsilon_b^{-1}) [J_1(GR) - \gamma J_1(\gamma GR)] \right. \\ \left. + (\varepsilon_{\parallel}^{-1} - \varepsilon_{\perp}^{-1}) [J_0(GR) - J_0(\gamma GR)] \right\}, & \mathbf{G} \neq 0. \end{cases} \quad (22)$$

The diagonal element $a_{yy}(\mathbf{G})$ is obtained from Eq. (22) by the replacement $\varepsilon_{\perp} \leftrightarrow \varepsilon_{\parallel}$.

In this section we consider solid cylinders, i.e. $\gamma \equiv 0$. The circles in Fig. 1 show the effective dielectric constant, given by Eq. (18), of the H -mode as a function of the filling fraction, $f = \pi R^2/A_c$, for uniaxial PC with a square lattice. The number of \mathbf{G} values (plane waves) considered in this calculation was 1200, which provided a good convergence in Eq. (18). The dielectric constant for the extra-ordinary mode (E -mode), Eq. (6) (shown by triangles in Fig. 1) is always larger than that for the ordinary wave (H -mode). Therefore, the effective medium is a uniaxial *positive* optically anisotropic crystal. To check the validity of the Maxwell-Garnett approximation, we plot in Fig. 1 (squares) the effective dielectric constant proposed in Ref. [12]

$$\varepsilon_{MG}^{(H)} = \frac{\varepsilon_{\parallel} + \Delta + f(\varepsilon_{\parallel} - \Delta)}{\varepsilon_{\parallel} + \Delta - f(\varepsilon_{\parallel} - \Delta)}. \quad (23)$$

Here $\Delta = \sqrt{\varepsilon_{\parallel}/\varepsilon_{\perp}}$. One can see that for all filling fractions the Maxwell-Garnett approximation gives overestimated values for the effective dielectric constant. For a very dilute system, $f < 0.07$, the Maxwell-Garnett approximation gives results that are practically indistinguishable from the exact ones (See insert in Fig. 1.). For the close-packed array of cylinders the Maxwell-Garnett approximation overestimates the dielectric constant by about 25%.

In Fig. 2 we plot two principal dielectric constants for the biaxial PC of solid carbon cylinders with a rectangular unit cell. The ratio of the sides of the rectangle is 1:2. The

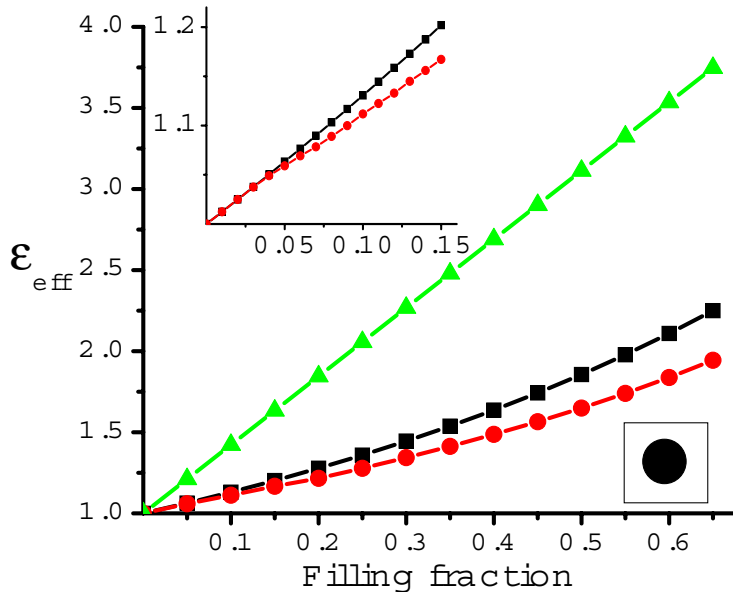


FIG. 1: In-plane effective dielectric constant for the H -mode for uniaxial PC of solid graphite cylinders with $\varepsilon_{\parallel} = 1.8225$ and $\varepsilon_{\perp} = 5.226$ in air, $\varepsilon_b = 1$ (circles). Straight line (triangles) is the effective dielectric constant for the E -mode, Eq. (7). The squares show the results of the Maxwell-Garnett approximation (23). Insert shows the region of small filling fractions.

difference between the two dielectric constants increases with the filling fraction, giving rise to a higher anisotropy of the corresponding effective medium. The Maxwell-Garnett approximation Eq. (23), which does not take into account the anisotropy of the unit cell, gives the values for ε_{MG} that lie between the two principal values, $\varepsilon_1 < \varepsilon_{MG} < \varepsilon_2$.

V. UNIAXIAL PHOTONIC CRYSTAL OF CARBON NANOTUBES

In our model we consider the carbon nanotubes as hollow graphite cylinders. In the experimental study⁸ of the dielectric properties of carbon nanotubes the outer radius of the cylinders was approximately $R = 5$ nm. The nanotubes formed a thin film and they were oriented along a specific direction. Although the nanotubes were not necessarily arranged periodically, one can assume that they formed almost a regular lattice, since the nanotube density is about 0.6 - 0.7 which is near the value of $f_c = \pi/4 \approx 0.785$ for a close-packed structure. Thus, the separation between the nanotubes (the period of the square lattice d) slightly exceeds $2R$, and in Ref. [12] it was estimated to be $d = 10.15$ nm. The inner radius $\gamma R = 0.25 - 2$ nm.¹² was evaluated from the amount of electromagnetic absorption for the E -polarized light. The four parameters f , R , γ , and $A_c = a^2$ are not independent

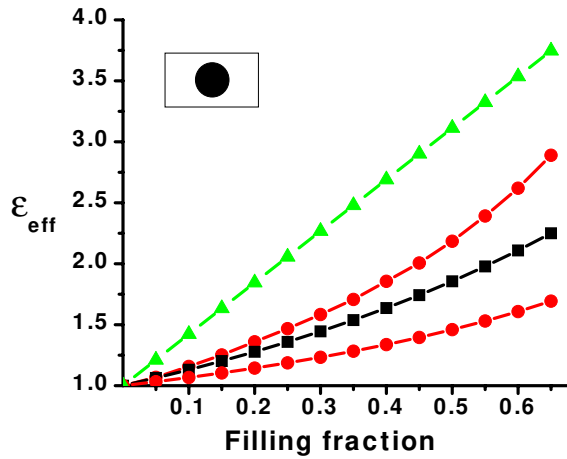


FIG. 2: A plot of the principal effective dielectric constants for the PC of solid carbon cylinders arranged in a rectangular lattice. The larger (smaller) dielectric constant ε_1 (ε_2) corresponds to the direction of the vector \mathbf{E} along the short (long) side of the rectangle. The Maxwell-Garnett dielectric constant is shown by the squares.

but related by the formula,

$$f = \pi R^2(1 - \gamma^2)/A_c. \quad (24)$$

Substituting the aforementioned parameters of the square unit cell into this formula allows one to check that they are self-consistent. It is worthwhile to mention that the background material in the experiment⁸ is not air but the host material Delrin or Teflon with $\varepsilon_b > 1$. Since neither the density of the host material nor its dielectric constant is known, one cannot expect very good agreement between the experimental results⁸ and theory. In all theoretical considerations it was assumed that $\varepsilon_b = 1$. Because of this lack of experimental data, the effective medium theories^{12,16} and the results shown in Fig. 1 give lower values for ε_{eff} than that observed in the experiment.⁸

It is obvious that the inner cavity reduces the permittivity of an isolated nanotube as compared to a solid graphite cylinder of the same size. It was argued¹² that for a periodic arrangement the effect of the inner cavity is less than that for a single cylinder and even can be ignored, if the ratio between the inner and outer radii γ does not exceed 0.4. This conclusion was supported by comparing the results of the Maxwell-Garnet approximation Eq. (23) and numerical band structure calculations. In Fig. 3 we plot the dielectric constant for a square lattice of hollow carbon nanotubes and compare the exact results obtained from

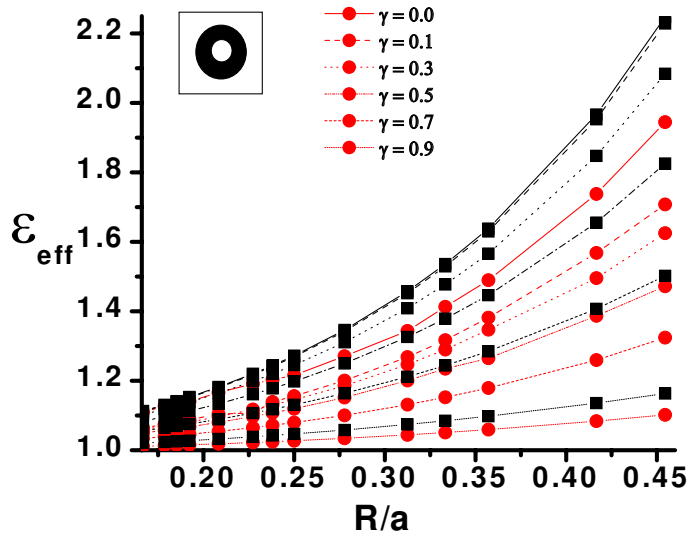


FIG. 3: The plot of the effective dielectric constant for square lattice of carbon nanotubes versus the outer radius for tubes with different ratios of the inner and outer radii, $\gamma = 0.1, 0.3, 0.5, 0.7$. The exact results are shown by circles and the results of the Maxwell-Garnett approximation are shown by squares.

Eqs. (18), (19), and (22) (shown by the circles) with the results given by the Maxwell-Garnett approximation (squares). One can see that, for the same outer radius, the effective dielectric constant drops with an increase of the inner radius. Thus, if the outer radius is fixed, the dependence on the inner radius cannot be ignored, even in the Maxwell-Garnett approximation. However, the effective dielectric constants exhibits much less sensitivity to the internal radius if it is plotted as a function of the filling fraction, Fig. 4. In the Maxwell-Garnett approximation (23) there is no dependence on the parameter γ , therefore, this approximation is represented by a single curve in Fig. 4. Here, only the total amount of the dielectric material is important, but not the topology of the cylinders. In the exact theory the effective dielectric constant depends on the details of the microstructure of the photonic crystal, but as far as the filling fraction is concerned, the topology plays a much less important role. Since the cylinder is uniquely determined by either two parameters out of three, R , γ , and f , the curves in Fig. 4 may cross each other. This means that at the crossing point the values of f and γ correspond to the same hollow cylinder. This can be easily seen from Eq. (24).

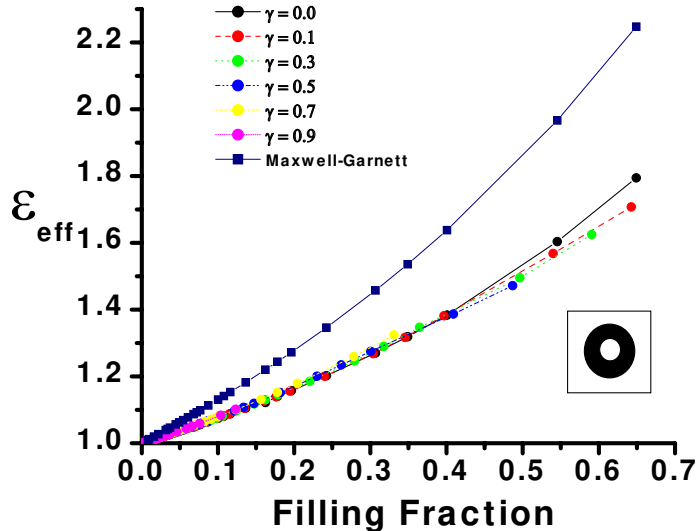


FIG. 4: A graph of the effective dielectric constant for a square lattice of carbon nanotubes versus filling fraction for tubes with different ratios of the inner and outer radii, $\gamma = 0.1, 0.3, 0.5, 0.7$. The exact results are shown by circles and the Maxwell-Garnett approximation is shown by squares.

VI. CONCLUSIONS

We calculated the low-frequency dielectric tensor for 2D photonic crystal of anisotropic parallel cylinders arranged in a periodic lattice in the perpendicular plane. The exact analytical formula for the principal values of the dielectric tensor was obtained. The results are applied for the periodic arrangement of carbon nanotubes which are rolled up from uniaxial graphite crystal with static values of the dielectric tensor $\varepsilon_{\parallel} = 1.8225$ and $\varepsilon_{\perp} = 5.226$. It was shown that the interior (vacuum) region of the nanotubes has a small effect on the dielectric properties of the photonic crystal and can be ignored. Although we are interested in the static dielectric tensor, it is clear that the developed long-wavelength limit approach remains valid, even for optical frequencies since the period of the lattice of carbon nanotubes $d = 10$ nm is much less than the optical wavelength $\lambda \approx 500$ nm. To calculate the dynamic dielectric tensor, one has to substitute in the general formula Eq. (16) the corresponding frequency-dependent values for ε_{\parallel} and ε_{\perp} . Of course at finite frequencies Eq. (16) gives the real part of the dielectric function. Calculations of the imaginary part require a generalization of the presented theory. This result will be reported elsewhere.

The exact theory presented here allows a calculation of the effective dielectric constant

of carbon nanotubes imbedded in a gas. Due to high absorbability of nanotubes, the concentration of gas in the interior region of the nanotubes may be different from that in the atmosphere. This leads to slightly different dielectric constants of the material in the interior and exterior regions of the cylinders. This effect can be registered by precise measurements of the shift of the resonant frequency of a resonant cavity.¹⁸ Thus, the proposed theory may find applications in the microwave detection of poisson gases in the atmosphere.

One more interesting application of carbon nantonube photonic crystal is related to its huge anisotropy of the effective dielectric constant. Recently Artigas and Torner¹⁰ demonstrated that the electromagnetic surface wave (Dyakonov wave¹¹) can propagate along the surface of a photonic crystal with high optical anisotropy. This wave propagates in a lossless dielectric medium and decays much slower than the surface plasmon. Since crystals with huge optical anisotropy are rare in nature, carbon nanotube photonic crystals may be considered as a promising material for integrated photonic circuits.

VII. ACKNOWLEDGEMENT

This work is supported by CONACyT (Mexico) Grant No. 42136-F.

-
- ¹ *Roadmap to Photonic Crystals*, ed. by S. Noda and T. Baba (Kluwer, Boston, 2003).
- ² E. Yablonovitch, *Phys. Rev. Lett.* **58**, 2059 (1987).
- ³ P. Kuchment, *The Mathematics of Photonic Crystals*, in: G. Bao, and L. Cowsar, Wen Masters (Eds.), *Mathematical Modeling in Optical Science*, Vol. 22, SIAM, Philidelphia, PA, 2001, pp. 207272; M. Birman and T. Suslina, *Operator Theory Adv. Appl.* **129**, 71 (2001).
- ⁴ *Heterogeneous Materials*, M. Sahimi, (Springer-Verlag, NY, 2003).
- ⁵ P. Halevi, A.A. Krokhin, and J. Arriaga, *Phys. Rev. Lett.* **82**, 719 (1999); A.A. Krokhin, P. Halevi, and J.Arriaga, *Phys. Rev. B* **65**, 115208 (2002).
- ⁶ S. Datta, C.T. Chan, K.M. Ho, and C.M. Soukoulis, *Phys. Rev. B* **48**, 14936 (1993).
- ⁷ A.A. Krokhin, and E. Reyes *Phys. Rev. Lett.* **93**, 023904 (2004).
- ⁸ W. A. de Heer, W. S. Bacsa, A. Châtelain, T. Gerfin, R. Humphrey-Baker, L. Forro, and D. Ugarte, *Science* **268**, 845 (1995); F. Bommeli, L. Degiorgi, P. Wachter, W.S. Bacsa, W.A. de

- Heer, and L. Forro, Solid St. Comm. **99**, 513 (1996).
- ⁹ I.H.H. Zabel, and D. Stroud, Phys. Rev. B **48** 5004 (1993); Zh.-Yu. Li, J. Wang, and B.-Yu. Gu *ibid* **58** 3721 (1998).
- ¹⁰ D. Artigas and L. Torner, Phys. Rev. Lett. **94** 013901 (2005).
- ¹¹ M.I. Dyakonov, Sov. Phys. JETP **67**, 714 (1988).
- ¹² F.J. García-Vidal, J.M Pitarke and J.B. Pendry, Phys. Rev. Lett. **78** 4289 (1997).
- ¹³ J.C. Maxwell-Garnett, *Philos. Trans. R. Soc.* **203**, 385 (1904).
- ¹⁴ M. Born and E. Wolf, *Principles of Optics*, (Pergamon Press, Oxford, 1975); L.D. Landau, E.M. Lifshitz, and L.P. Pitaevskii, *Electrodynamics of Continuous Media*, 2nd ed., (Pergamon, Oxford, 1984).
- ¹⁵ *Handbook of Optical Constant of Solids*, Edited by E.D. Palik (Academic, Orlando, 1991).
- ¹⁶ W. Lü, J. Dong, and Z.-Y. Li, Phys. Rev. B **63**, 033401 (2000); K. Kempa, *et al.*, Nano Lett. **3**, 13 (2003).
- ¹⁷ P. Wu, B. Kimball, J. Carlson, and D. Rao, Phys. Rev. Lett. **93**, 013902 (2004).
- ¹⁸ A. Anand, J. A. Roberts, F. Naab, J.N. Dahiya, O.W. Holland, and F.D. McDaniel, *Select Gas Absorption in Carbon Nanotubes Loading a Resonant Cavity to Sence Airborne Toxins Gases*, Nuclear Instruments and Methods B (Elsivier, 2005).